Hindawi
Journal of Nanomaterials
Volume 2022, Article ID 9652966, 13 pages
https://doi.org/10.1155/2022/9652966

Research Article

Mechanical Behavior of Helical Spring Made of Composite with and without Material Property Grading under Stable Load

Saeed Asiri

King Abdulaziz University, Faculty of Engineering, Mechanical Engineering Department, Jeddah, Saudi Arabia

Correspondence should be addressed to Saeed Asiri; sasiri@kau.edu.sa

Received 16 February 2022; Revised 3 March 2022; Accepted 8 March 2022; Published 21 March 2022

Academic Editor: Palanivel Velmurugan

Springs are one of the most popular means of mechanically storing and issuing energy, and they can be found in a wide variety of machines and products. Most springs are made of metal, and nowadays, there are many new alloys to choose from, but nonmetallic materials, such as the reinforced plastics and ceramics, have been appearing worldwide. The research problem is the performance for circular cross-sectional springs with the same geometry and manufactured with three different materials: steel, composite, and functionally graded material (FGM) under stable loading using finite element analysis. This paper intends to guide mechanical designers in considering different material options for a spring design as well as to provide a methodology through finite element analysis for selecting the most favorable material option for the application required. The findings of this research show that some feature performances of compression springs made of carbon steel are improved by using FGM and composite materials. Enhanced capabilities include higher load to failure: 1.48 times in an FGM spring and 1.1 times in a composite spring, as well as increased energy storage: 1.53 times in an FGM spring and 6.84 times in a composite spring and less weight representing only 61% in an FGM spring and 24% in a composite spring.

1. Introduction

Springs are one of the most popular means of mechanically storing and issuing energy, and they can be found in a wide variety of machines and products. Most springs are made of metal, and nowadays, there are many new alloys to choose from, but nonmetallic materials, such as the reinforced plastics and the ceramics, have been appearing worldwide.

The research aim focuses on contributing to the mechanical design of a spring considering the selection of its manufacturing material. In this sense, it will carry out an analysis of two springs made with two new types of materials used worldwide for manufacturing them, comparing the performance of a spring made of FGM with a spring made of composite materials, and these results will be contrasted with a traditional spring made of carbon steel. For completing the evaluation, a finite element analysis will be carried out using the commercial software ANSYS Workbench. Three computational cases will be performed with the same geometric model of a helical spring of circular cross section and subjected to compression. It will vary only on the material used in each computational case; for comparing the spring performance made of each of three materials analyzed in this study, FGM, composite material, and carbon steel were used.

First, it will corroborate the computational model of carbon steel spring, comparing the finite element analysis (FEA) results with mathematical models of spring design from [1]. Then, it will validate the computational model of a carbon fiber spring (composite materials) considering the experimental results published in the international literature. These validations will allow corroborating the methodology used for the FEA of each of the cases assessed in this study and will ensure the reliability of the results issued.

2. Methodology

The following phases were considered for the numerical analysis of circular cross-sectional spring with steel, FGM, and composite materials.

(i) Validation analysis

(ii) Computational models

2.1. Validation Analysis. Some researchers [2–6] have demonstrated that the mechanical behavior of composite materials, as well as FGM, can be simulated satisfactorily. This research intends to simulate the mechanical behavior of three springs taking into account several experimental research results as well as international standards to demonstrate the reliability of the FEA results in the present investigation.

According to [1, 7], the design calculation for steel spring in the case of compression load without initial tension refers to the following equations.

2.1.1. Deflection of Spring δ.

$$\delta = \frac{8N_a D^3 P}{Gd^4}, \tag{1}$$

where N_a is the number of active coils or number of active turns, D is the mean diameter of coil $D = (D_i + D_o)/2$ (mm), P is the load (force) acting on spring (N), G is the G modulus of rigidity (7.85×10^4 N/mm^2 for steel spring), and d is the diameter of the material (mm).

2.1.2. Spring Constant (k).

$$k = \frac{P}{\delta}. \tag{2}$$

2.1.3. Energy Stored in Spring (U).

$$U = \frac{P\delta}{2}. \tag{3}$$

Equation (1) will be used to validate the deflection result of the numerical analysis in the case of a steel spring with a circular cross section.

Equations (2) and (3) will be used to evaluate the spring performance in each of the three cases assessed in this study.

2.1.4. Composite Spring. According to [8], develop an experimental investigation into the mechanical behaviors of helical composite springs made of preimpregnated fibers fabricated with fibers along with ±45° directions. Then, pack, coil, and outer braid one layer with resin-impregnated 3K carbon fiber. The present paper will focus only on the "BU" preformed composite bar structure shown by [8] (see Figure 1).

The experimental results of this research [8] considering a cylindrical helical spring with a square cross section will be used in this paper only for validation purpose to corroborate the mechanical behavior of the composite spring made of 3K carbon fiber outer braid with a "BU" preformed structure.

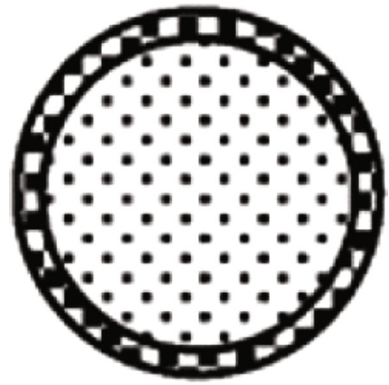

Figure 1: 3K carbon fiber outer braid (one layer): 37.5 cm of length.

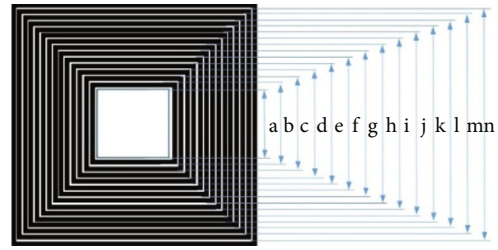

Figure 2: Geometrical dimensions of the square cross section for the validation of composite spring.

Figure 2 and Table 1 show the geometrical dimensions of the square cross section for the computational model used in the validation of composite spring.

Considering the manufacturing methodology of carbon fiber composite spring described by [8], Figure 2 shows the square cross-sectional compound for a core made of preimpregnated fibers fabricated with fibers along with ±45° directions with an outer braided one layer of 3K carbon fiber. This 3K carbon fiber lamina with a length of 37.5 cm is coiled 14 times, as shown in Table 1.

The total side length of the square cross section is 10 mm, after coiling 14 times the 3K carbon fiber lamina according to the description in Table 1 and considering a carbon fiber lamina thickness of 0.22 mm. Table 2 shows the properties of 3K carbon fiber that were used in the numerical simulation.

Figure 3(a) shows the experimental investigation spring model [8] in comparison with the geometrical model developed in the module ACP (pre) from ANSYS Workbench of the composite spring used for validation purposes (Figure 3(b)).

Considering the maximum compression load in the elastic range of the spring (250 kgf or 2452 N) obtained experimentally by [8]. Figure 4 shows the boundary conditions and mesh used in the numerical simulation. Spring mesh was refined until achieving the convergence. The final mesh sizing was 0.8 mm (0.031 in) using second-order solid elements.

Table 1: Geometrical dimensions of the square cross section for the validation of composite spring.

Lamina coiled	Square cross section (Figure 2)	Side length of square cross section (mm)	Perimeter (mm)	Carbon fiber lamina total length (cm)
1	a	3.84	15.36	37.5
2	b	4.28	17.12	
3	c	4.72	18.88	
4	d	5.16	20.64	
5	e	5.60	22.40	
6	f	6.04	24.16	
7	g	6.48	25.92	
8	h	6.92	27.68	
9	i	7.36	29.44	
10	j	7.80	31.20	
11	k	8.24	32.96	
12	l	8.68	34.72	
13	m	9.12	36.48	
14	n	9.56	38.24	

Table 2: 3K carbon fiber properties.

Tow size k	Filament properties					Minimum carbon content (%)
	Tensile strength (GPa)	Young's modulus (GPa)	Diameter (μ m)	Elongation (%)	Density (g cm^{-3})	
3	3.75	231	7.0	1.4	1.76	92

Source: [9].

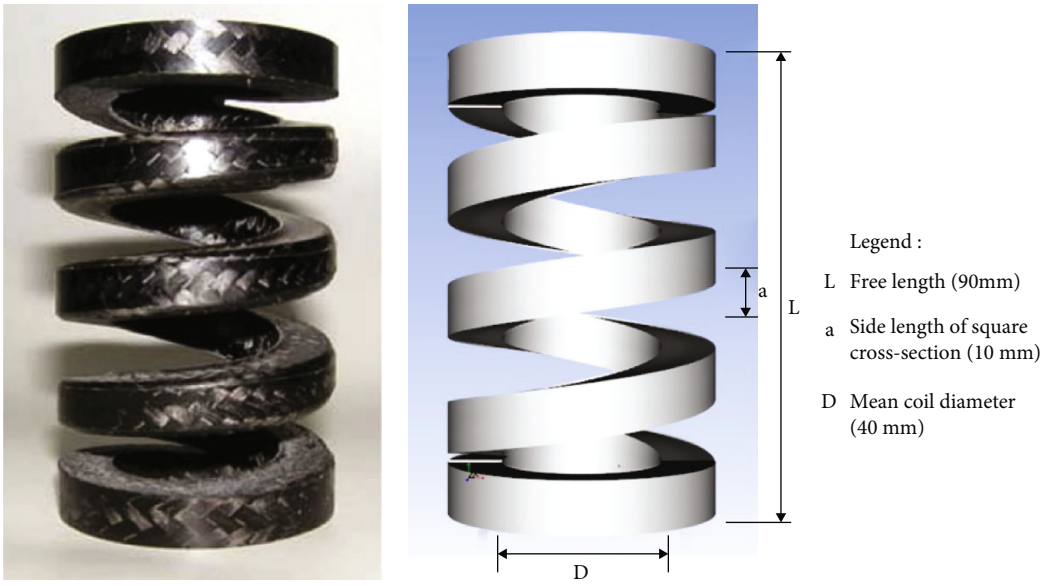

Source : Chiu C, et al. 2007

(a) Experimental investigation spring model

(b) Numerical simulation spring model

Figure 3: Geometric comparison between the real coil spring and the computational model.

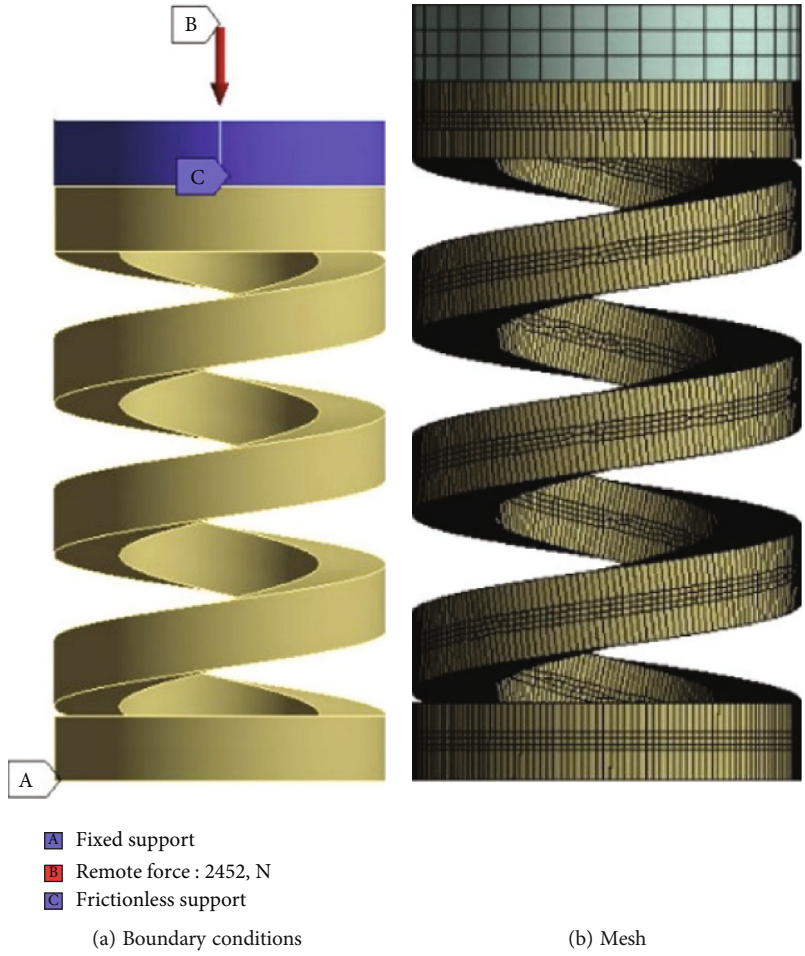

(a) Boundary conditions (b) Mesh

Figure 4: Boundary conditions and mesh of the computational model for validation purpose.

Another aspect for validating is the failure load in the elastic range for the composite spring; hence, it will consider the results obtained experimentally by [8] related to the failure behavior of this coil spring.

2.2. Computational Models. After validating the methodology used for simulating, three geometric models were carried out using ANSYS Workbench considering the following general features described in Table 3.

2.2.1. Computational Model 1. Mechanical and physical properties of the material (carbon steel with C ≤ 0.3%) used for numerical simulation are shown in Table 4.

Figure 5 depicts the boundary conditions and mesh used in computational model 1. It highlighted a load compression force of 981 N (220.54 lbf), which is the maximum load in the elastic range.

2.2.2. Computational Model 2. Figure 6 shows the difference in compositions and properties between an ordinary composite material and FGM. There is a distinct interface between metals and ceramics in an ordinary composite material, but not in an FGM. This difference corresponds to the distribution of properties. An ordinary composite material contains a sudden change in properties at the interface, while an FGM presents a gradual change inside it.

For developing the numerical simulation of the FGM compound by carbon steel with less than 0.5% of C in addition with aluminum oxide (Al_2O_3), the research developed by [13] was considered, as well as [14, 15] to determine the material properties [14]. Describe that properties (P) are dependent on the temperature and are expressed in the form

$$P = P_0\left(\frac{P_{-1}}{T} + 1 + P_1\,T + P_2\,T^2 + P_3 T^3\right), \tag{4}$$

where P_0, P_1, P_2, and P_3 are constants in the cubic fit of the material property and T is the temperature in kelvin. For this paper, T is equivalent to 298 K.

Besides, reference [14] states that, to model the material properties of FGM effectively, the properties must be both temperature-dependent and position-dependent. The combination of these functions gives rise to the effective material properties of FGMs and is expressed as

$$P_{\text{eff}}(T,\xi) = P_{\text{m}}(T)V_{\text{m}}(\xi) + P_{\text{c}}(T)(1 - V_{\text{m}}(\xi)), \tag{5}$$

Table 3: General features of computational models.

Feature	Computational model		
	1	2	3
Material	Carbon steel C ≤ 0.3%	FGM (carbon steel C ≤ 0.3% + A l_2O_3)	Composite material (resin epoxy + 3K carbon fiber)
Shape of spring*	Helical coil, both end grounded	Helical coil, both end grounded	Helical coil, both flat end unground
Cross-sectional shape	Circular	Circular	Circular
Free length (mm)	90	90	90
Cross-sectional diameter (mm)	10	10	10
Mean coil diameter (mm)	40	40	40
Number of active coils	3.6	3.6	3.6
Type of load applied	Compression	Compression	Compression
Type of finite element	2nd order solid element	2nd order solid element	2nd order solid element
Size of element (mm)	0.8	0.8	0.8

*According to [10].

Table 4: Mechanical and physical properties of carbon steel with C ≤ 0.3%.

Property	Value
Density (kg/m^3)	7850
Young's modulus (GPa)	201
Poisson's ratio	0.3
Tensile yield strength (MPa)	250
Compressive yield strength (MPa)	250

Source: [11].

where P_{eff} is the effective material property of FGM, P_m and P_c are the temperature-dependent properties of the metal and ceramic, respectively, and V_m is the volume fraction of the metal constituent of the FGM. In addition, reference [14] mentions that a simple power-law exponent of the volume fraction distribution is used to provide a measure of the amount of metal in FGMs. For an axisymmetric cylinder, the expression for the volume fraction of ceramic is

$$V_c = \left(\frac{r - r_i}{r_o - r_i}\right), \quad (6)$$

where r_o is the outer radius of the cylinder, r_i is the inner radius, r is the radial coordinate ($r_i \le r \le r_o$), and n is the power-law index ($0 \le n \le \infty$).

According to the preceding distribution, the outer surface of the cylinder is ceramic-rich and the inner surface is metal-rich. Table 5 shows the modulus of elasticity of aluminum oxide (Al_2O_3) in Pa, considering Equation (4). Table 6 shows the Poisson's ratio of aluminum oxide (Al_2O_3), considering Equation (4).

For this paper, it was considered a power-law index (n) equivalent to 1. In this case, the mechanical and physical properties of the FGM compound by carbon steel with less than 0.5% of C in addition with aluminum oxide (Al_2O_3) and considering Equations (4)–(6) are shown in Table 7.

According to [16], develop an algorithm to simulate properties of FGM for the design optimization in a dental implant for bone remodeling. In this sense and to estimate the mechanical and physical properties, which are position-dependent, an algorithm was developed to simulate this computational model in the ANSYS Workbench.

Figure 7 depicts the boundary conditions and mesh used in computational model 2. It highlighted a load compression force of 1450 N (325.97 lbf), which is the maximum load in the elastic range.

2.2.3. Computational Model 3. Considering the same methodology explained in Section 2.1 about the validation of composite spring simulation, Figure 8 shows the geometrical dimensions of the circular cross section for computational model 3.

Table 8 shows the geometrical dimensions of the circular cross section for computational model 3.

The final diameter of the circular cross section is 10 mm, after coil 14 times the 3K carbon fiber lamina according to the description in Table 8 and considering a carbon fiber lamina thickness of 0.22 mm. Table 2 shows the properties of 3K carbon fiber that will be used in the numerical simulation.

Figure 9 depicts the boundary conditions and mesh used in computational model 3. It highlighted a load compression force of 1070 N (240.55 lbf), which is the maximum load in the elastic range.

3. Results and Discussion

3.1. Validation Analysis. Figure 10 shows the maximum displacement in the elastic range for the carbon steel spring considering a compression load of 981 N (220.54 lbf).

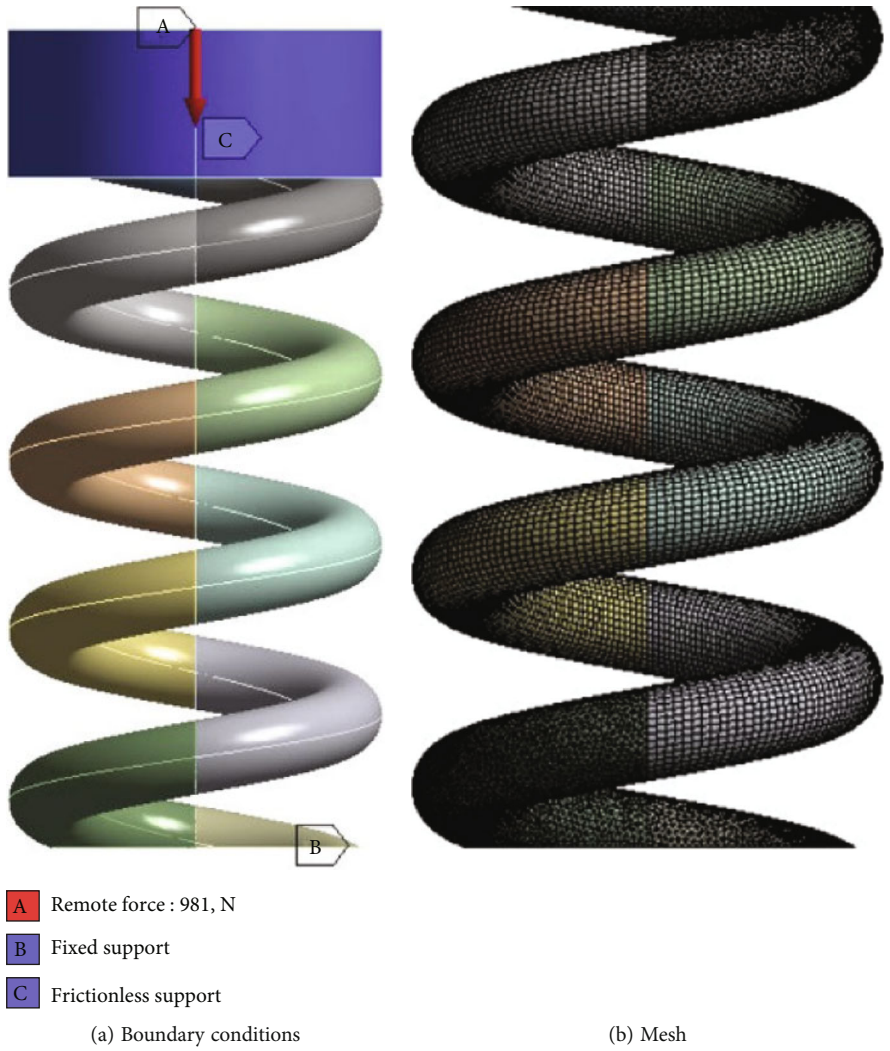

Figure 5: Boundary conditions and mesh of the computational model 1.

Equation (1) represents the deflection of the spring according to international standard [1]. Considering Equation (1), the theoretical maximum deflection in the elastic range for the carbon steel spring is 2.3 mm, and the FEA result in Figure 10 shows a maximum displacement equivalent to 2.4 mm; in consequence, the relative error is 4.19%. Hence, results about displacement demonstrate that numerical simulation of the steel spring can represent very well the spring theoretical behavior. Figure 11 shows the maximum displacement in the elastic range for the composite spring with a square cross section.

Considering the data issued by [8], the maximum deflection for the composite spring during the experiment in the elastic range is 16.23 mm, and the FEA result in Figure 11 shows a maximum displacement equivalent to 17.12 mm; hence, the relative error is 5.48%.

When the experimental behavior of failure (Figure 12(b)) is compared with results obtained by FEA (Figure 12(a)), it can be noticed that there is a correspondence in the failure location.

The maximum stress ratio (1.2) in FEA results matches the experimental location of a crack at the opening end of the coil spring. With this compressive load (1452 N), the spring in the numerical simulation exhibits an orange color in most coils of spring that represent a stress ratio near to one, being the value of 1 the limit of the stress ratio for the failure in the elastic range. Stress ratio values equal to or more than one represent a failure by yield strength.

In consequence, results about not only displacement but also failure behavior demonstrate that numerical simulation of the composite spring can represent very well the composite spring behavior during experimental investigation.

3.2. Computational Models

3.2.1. Computational Model 1. Figure 10 shows the steel spring maximum displacement in the elastic range, and this displacement was validated with Equations (1) and (2) that represents the theoretical behavior.

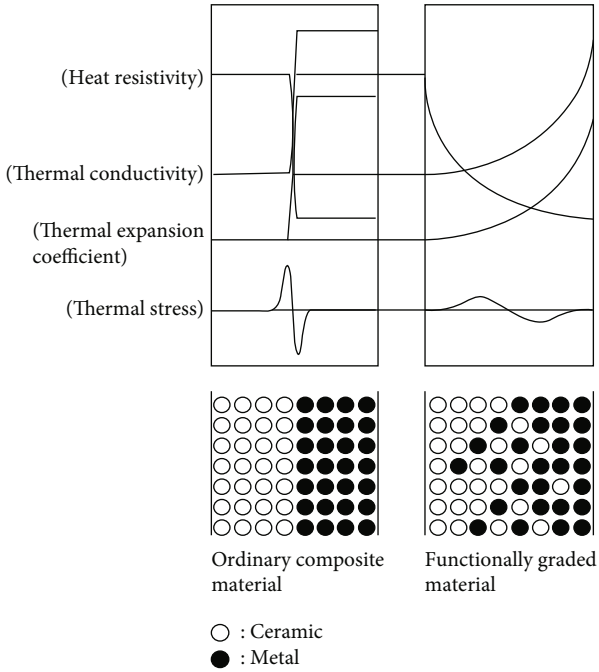

Figure 6: Material structures and properties of ordinary composite and FGM. Source: [12] Handbook of Advanced Ceramics.

Table 5: Modulus of elasticity of aluminum oxide (Al_2O_3).

P_0	P_{-1}	P_1	P_2	P_3
349.55×10^9	0	-3.853×10^{-4}	4.027×10^{-7}	-1.673×10^{-10}

Source: [14].

Table 6: Poisson's ratio of aluminum oxide (Al_2O_3).

P_0	P_{-1}	P_1	P_2	P_3
0.2600	0	0	0	0

Source: [14].

Table 7: Mechanical and physical properties of FGM.

Property	Value
Density (kg/m^3)	$7850(1 - r/r_0) + 3800(r/r_0)$
Young's modulus (Pa)	$2.01 \times 10^{11}(1 - r/r_0) + 3.204 \times 10^{11}(r/r_0)$
Poisson's ratio	$0.3(1 - r/r_0) + 0.26(r/r_0)$
Tensile yield strength (Pa)	$2.5 \times 10^8(1 - r/r_0) + 4 \times 10^8(r/r_0)$
Compressive yield strength (Pa)	$2.5 \times 10^8(1 - r/r_0) + 4 \times 10^8(r/r_0)$

Figure 13 exhibits the stress ratio obtained in the numerical simulation, considering that stress ratio equivalent or more than 1 represents the failure in the elastic range of the material.

In this case, Figure 13 shows a maximum stress ratio equivalent to 1.025, which means that the material reaches the yield strength; hence, the compression load used in this numerical simulation (981 N) is considered as the maximum load in the elastic range.

3.2.2. Computational Model 2. Figure 14 shows the FGM spring maximum displacement in the elastic range. It can be noticed that a maximum displacement is equivalent to 2.48 mm considering a compressive load of 1450 N (325.97 lbf).

Figure 15 shows the stress ratio obtained in the numerical simulation, with a maximum stress ratio equivalent to 1.03; it means that the material reaches the yield strength; hence, the compression load used in this numerical simulation (1450 N) is considered as the maximum load in the elastic range.

3.2.3. Computational Model 3. Figure 16 exhibits the composite spring maximum displacement in the elastic range. It can be noticed that a maximum displacement is equivalent to 15.07 mm (0.59 in) considering a compressive load of 1070 N (240.55 lbf).

Figure 17 shows the stress ratio obtained in the numerical simulation, obtaining a maximum stress ratio equivalent to 1.05; it means that the material reaches the yield strength; hence, the compression load used in this numerical simulation (1070 N) is considered as the maximum load in the elastic range.

Table 9 shows the performance comparison between these three computational models, which will help to better understand how new development in materials such as FGM and composite can enhance the capability and potential use of springs.

As shown in Table 9, springs made of FGM and composite outperform springs made of carbon steel in some characteristics. Regarding load-to-failure performance, an FGM

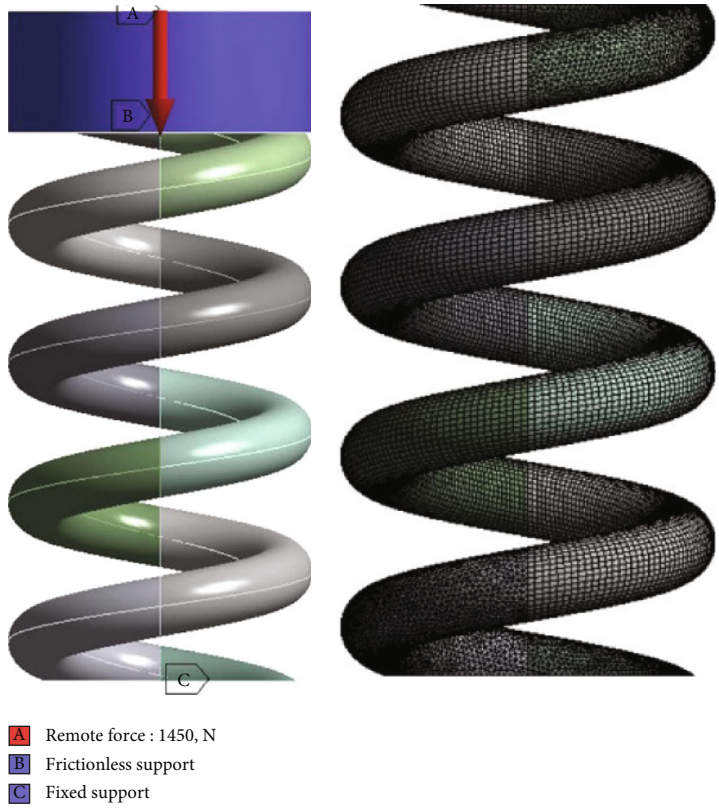

(a) Boundary conditions (b) Mesh

Figure 7: Boundary conditions and mesh of computational model 2.

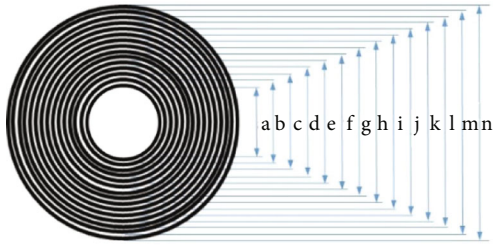

Figure 8: Geometrical dimensions of the circular cross section for computational model 3.

Table 8: Geometrical dimensions of the circular cross section for computational model 3.

Lamina coiled	Circular cross section (Figure 8)	Circular cross-sectional diameter (mm)	Total length of carbon fiber lamina (cm)
1	a	3.84	29.5
2	b	4.28	
3	c	4.72	
4	d	5.16	
5	e	5.60	
6	f	6.04	
7	g	6.48	
8	h	6.92	
9	i	7.36	
10	j	7.80	
11	k	8.24	
12	l	8.68	
13	m	9.12	
14	n	9.56	

spring outperforms a carbon steel spring 1.48 times, while a carbon fiber spring outperforms its carbon steel counterpart by 1.1 times.

Regarding weight and for industrial applications that require it, such as in the manufacturing of vehicles and automobiles [17, 18], this performance characteristic also shows its advantages for FGM and composite springs. As shown in Table 9, the weight of an FGM spring represents only 61% of the mass of a carbon steel spring, while its similar one made of composite has a weight equivalent to 24% of the weight carbon steel spring [19–21].

Another favorable feature is about the energy storage in the coil spring, where again both springs, FGM and composite, outperform their carbon steel counterpart by 1.53 times and 6.84 times, respectively. In the same sense, the characteristic about specific energy stored in the coil spring that relates the energy stored in the spring with the weight of

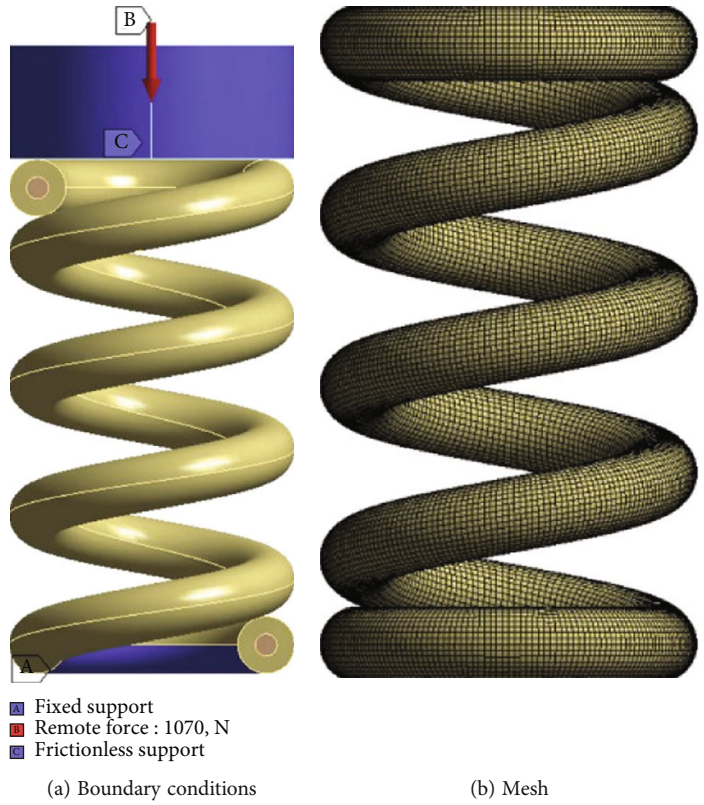

(a) Boundary conditions (b) Mesh

Figure 9: Boundary conditions and mesh of computational model 3.

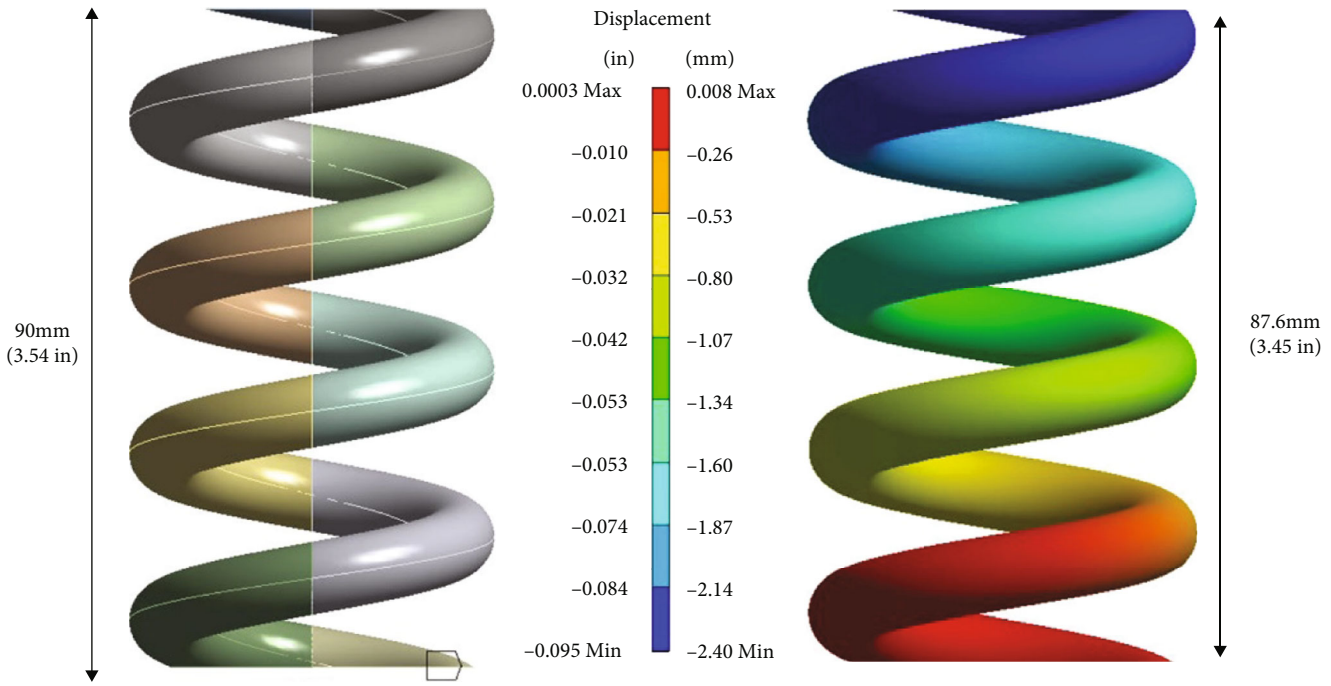

(b) Final condition (a) Initial conditions

Figure 10: Steel spring maximum displacement in the elastic range.

the spring demonstrates that a composite spring can store more energy per mass unity, 11.3 times more than an FGM spring and 28.2 times more than a steel spring.

On the other hand, for applications that require high stiffness or higher spring constant, the best option is an FGM spring, followed by a carbon steel spring, and at last

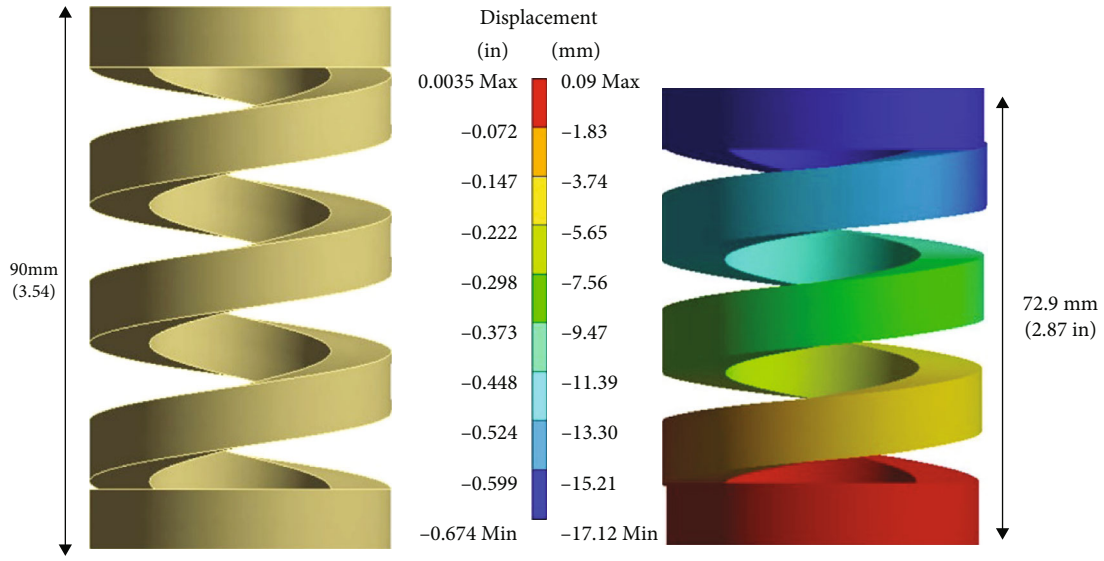

(a) Initial conditions (b) Final condition

Figure 11: Composite spring maximum displacement in the elastic range.

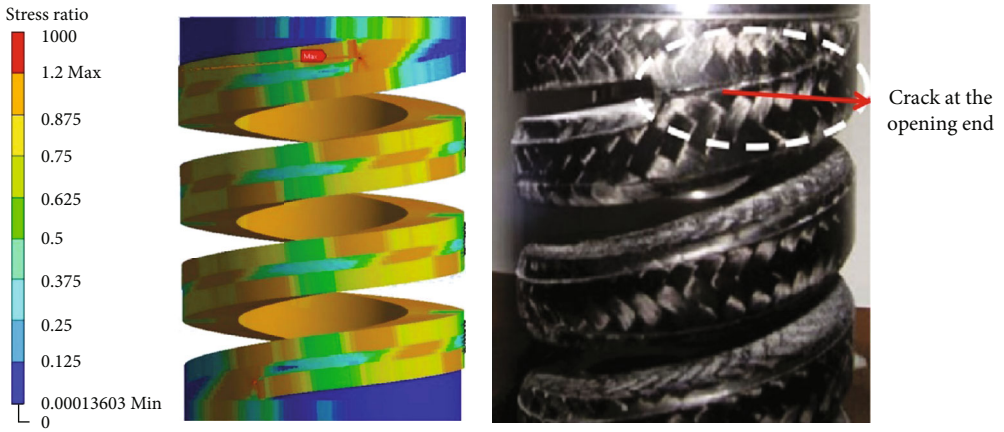

Source : Chiu C, et al al. 2007

(a) Numerical simulation of failure (b) Experimental behavior of failure

Figure 12: Comparison of failure between FEA simulation and experimental behavior of composite spring.

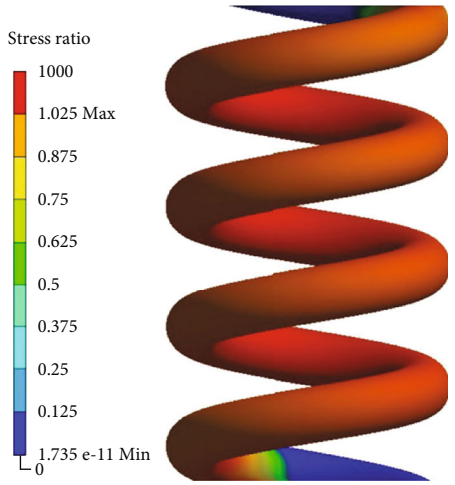

Figure 13: Failure at maximum displacement in the elastic range for computational model 1.

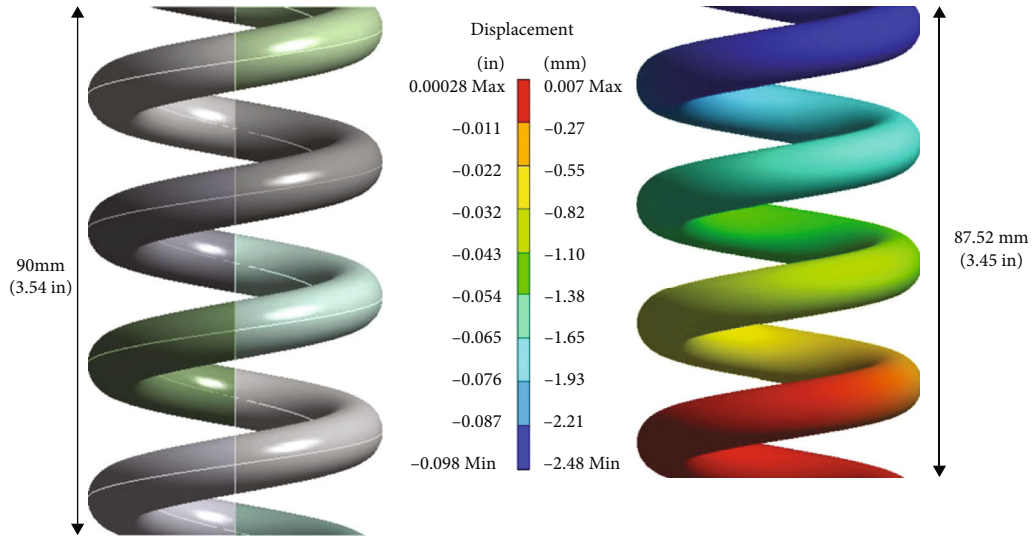

(a) Initial conditions (b) Final condition

Figure 14: Maximum displacement in the elastic range for computational model 2.

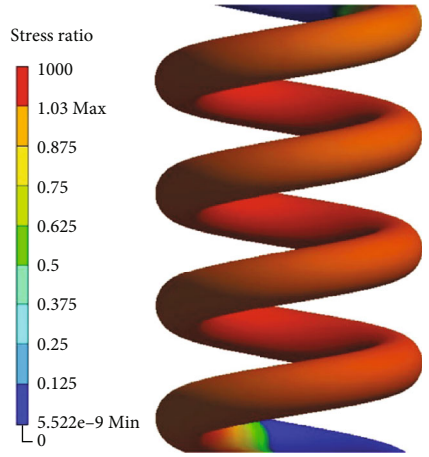

Figure 15: Failure at maximum displacement in the elastic range for computational model 2.

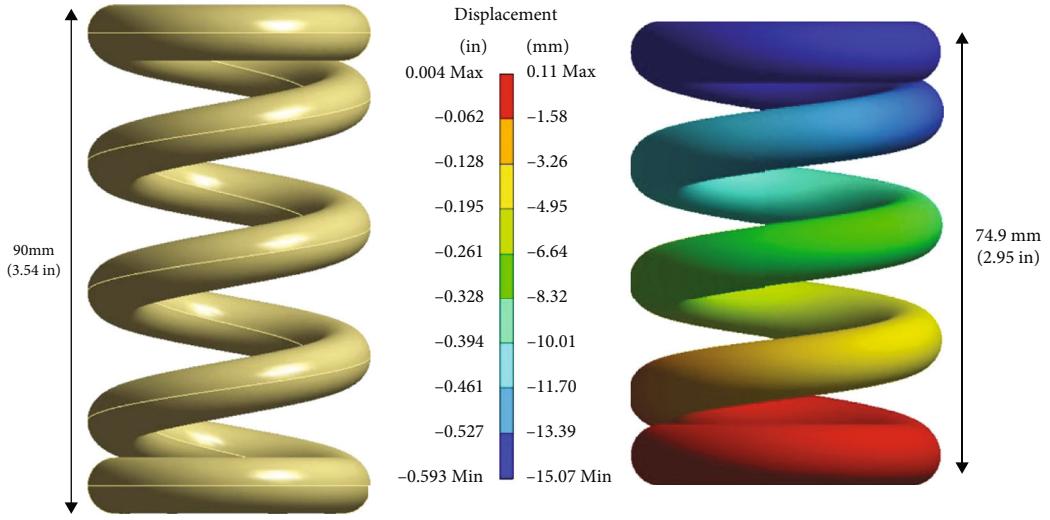

(a) Initial conditions (b) Final condition

Figure 16: Maximum displacement in the elastic range for computational model 3.

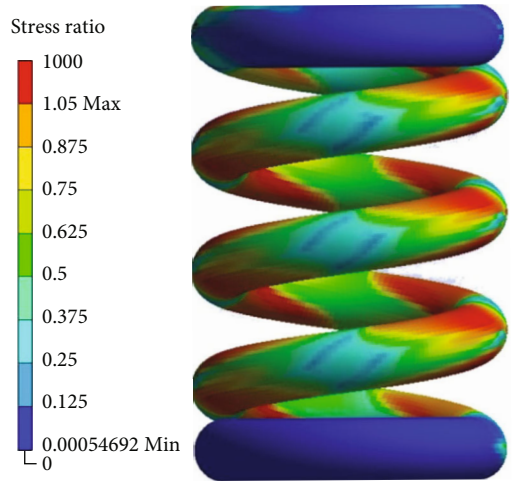

Figure 17: Failure at maximum displacement in the elastic range for computational model 3.

Table 9: Comparison of spring performance.

Computational model	1 (plain steel)	2 (FGM)	3 (composite)
Failure load (N)	981	1450	1070
Deflection δ (mm)	2.40	2.48	15.07
Spring constant k (N/mm)	408.75	584.68	71.00
Weight of spring (g)	307.0	187.7	74.6
Energy stored in spring U (J)	1177.20	1798.00	8052.45
Specific energy stored in spring (J/g)	3.83	9.58	108.07

a composite material spring. This characteristic intrinsically linked to the deflection of the spring is modifiable in a composite material spring by selecting laminates of carbon fiber with mechanical properties superior to those used in the present work [22, 23].

4. Conclusions

Three computational models were carried out to compare the spring performance considering three different kinds of materials: carbon steel, FGM compound by carbon steel+aluminum oxide, and composite material. Validation of these computational models was confirmed considering international standards and international publications.

The results of this work show that some feature performances of compression springs made of carbon steel are improved when using FGM and composite materials. Enhanced capabilities include higher load to failure (1.48 times in an FGM spring and 1.1 times in a composite spring) as well as increased energy storage (1.53 times in an FGM spring and 6.84 times in a composite spring) and less weight (representing 61% in weight in an FGM spring and 24% in a composite spring).

Data Availability

The data used to support the findings of this study are included within the article.

Conflicts of Interest

The author declares that there are no conflicts of interest.

References

[1] C. Zhao, L. Ren, Z. Song, L. Deng, and Q. Liu, "A study on the tubular composite with tunable compression mechanical behavior inspired by wood cell," *Journal of the Mechanical Behavior of Biomedical Materials*, vol. 89, pp. 132–142, 2019.

[2] L. Wu, L. Chen, H. Fu, Q. Jiang, X. Wu, and Y. Tang, "Carbon fiber composite multistrand helical springs with adjustable spring constant: design and mechanism studies," *Journal of Materials Research and Technology*, vol. 9, no. 3, pp. 5067–5076, 2020.

[3] J. Ke, Z. Y. Wu, Y. S. Liu, Z. Xiang, and X. D. Hu, "Design method, performance investigation and manufacturing process of composite helical springs: a review," *Composite Structures*, vol. 252, article 112747, 2020.

[4] M. Rashad, M. Wahab, and T. Y. Yang, "Experimental and numerical investigation of RC sandwich panels with helical springs under free air blast loads," *Steel and Composite Structures*, vol. 30, no. 3, pp. 217–230, 2019.

[5] Z. H. A. N. Bowen, S. U. N. Lingyu, H. U. A. N. G. Bincheng, Z. H. A. O. Guanbo, and W. A. N. G. Qian, "Design and optimization of automotive composite helical spring," *Journal of Beijing University of Aeronautics and Astronautics*, vol. 44, no. 7, p. 1520, 2018.

[6] Q. Jiang, Y. Qiao, F. Zhao et al., "Composite helical spring with skin-core structure: Structural design and compression property evaluation," *Polymer Composites*, vol. 42, no. 3, pp. 1292–1304, 2020.

[7] A. Abdullah Hamad, M. Lellis Thivagar, M. Bader Alazzam et al., "Dynamic systems enhanced by electronic circuits on 7D," *Advances in Materials Science and Engineering*, vol. 2021, Article ID 8148772, 11 pages, 2021.

[8] C. Chiu, C. Hwan, H. Tsai, and W. Lee, "An experimental investigation into the mechanical behaviors of helical composite springs," *Composite Structures*, vol. 77, no. 3, pp. 331–340, 2007.

[9] P. Morgan, *Carbon fibers and their composites*, Taylor & Francis Group, Boca Raton, FL, USA, 2005.

[10] JIS: Japanese Industrial Standard, *Coil springs-part 2: expression of the specification on helical compression springs*, 2009.

[11] ASME, "ASME Boiler & Pressure Vessel Code," in *Section II Part D, Properties-Material ASME*, ASME, New York, USA, 2017.

[12] S. Somiya, *Handbook of Advanced Ceramics. Materials, Applications, Processing, and Properties*, Academic Press, 2013.

[13] M. Naebe and K. Shirvanimoghaddam, "Functionally graded materials: a review of fabrication and properties," *Applied Materials Today*, vol. 5, no. 2016, pp. 223–245, 2016.

[14] J. N. Reddy and C. D. Chin, "Thermomechanical analysis of functionally graded cylinders and plates," *Journal of Thermal Stresses*, vol. 21, no. 1998, pp. 593–626, 1998.

[15] H. Shen, *Functionally graded materials: nonlinear analysis of plates and shells*, CRC Press. Taylor & Francis Group, 2009.

[16] D. Lin, Q. Li, W. Li, S. Zhou, and M. Swain, "Design optimization of functionally graded dental implant for bone remodeling," *Composites Part B*, vol. 40, no. 2009, pp. 668–675, 2009.

[17] E. R. Van Norman and D. C. Parker, "A comparison of common and novel curriculum-based measurement of reading decision rules to predict spring performance for students receiving supplemental interventions," *Assessment for Effective Intervention*, vol. 43, no. 2, pp. 110–120, 2018.

[18] M. Bader Alazzam, H. Mansour, M. M. Hammam et al., "Machine learning of medical applications involving complicated proteins and genetic measurements," *Computational Intelligence and Neuroscience*, vol. 2021, Article ID 1094054, 6 pages, 2021.

[19] T. W. Liu, J. B. Bai, Q. H. Lin, and Q. Cong, "An analytical model for predicting compressive behaviour of composite helical structures: considering geometric nonlinearity effect," *Composite Structures*, vol. 255, article 112908, 2021.

[20] M. B. Alazzam, H. Mansour, F. Alassery, and A. Almulihi, "Machine learning implementation of a diabetic patient monitoring system using interactive E-app," *Computational Intelligence and Neuroscience*, vol. 2021, Article ID 5759184, 7 pages, 2021.

[21] G. Apsar, M. Musthak, and J. Ahmed, "Study of factors affecting tape-wound composite helical spring prepared by E-glass/epoxy by using Taguchi method and statistical distributions," *International Journal of Composite Materials*, vol. 10, no. 1, pp. 10–17, 2020.

[22] M. B. Alazzam, F. Hajjej, A. S. AlGhamdi, S. Ayouni, and M. A. Rahman, "Mechanics of materials natural fibers technology on thermal properties of polymer," *Advances in Materials Science and Engineering*, vol. 2022, Article ID 7774180, 5 pages, 2022.

[23] R. A. Kshirsagar, S. S. Gaonkar, S. M. Pandharpure, D. Desale, and S. K. Gorave, "Design and analysis of wave spring," *Journal of Emerging Technologies and Innovation Research (JETIR)*, vol. 6, no. 4, 2019.